water

Article

Experimental Analysis on Hanging Dam Formation and Evolution

Randula Senarathbandara *, Shawn P. Clark and Karen Dow

Department of Civil Engineering, University of Manitoba, 66 Chancellor Circle, Winnipeg, MB R3T 2N2, Canada; shawn.clark@umanitoba.ca (S.P.C.); karen.dow@umanitoba.ca (K.D.)
* Correspondence: randulas@myumanitoba.ca; Tel.: +1-204-801-5940

Abstract: Hanging dams are thick accumulations of frazil ice beneath an existing ice cover that are formed during the freeze-up period at locations where a fast-flowing river section enters a section with relatively low velocity. Hanging dams can have a substantial impact on the hydraulics of an ice-covered river. This paper presents an experimental study on hanging dam formation and evolution conducted using a laboratory physical model of a river issuing water into a relatively large reservoir using simulated frazil ice and a simulated ice cover. The incoming ice supply rate and the approach Froude number of the river are the two parameters that have an impact on the hanging dam formation with respect to several physical characteristics of the hanging dam. Hanging dam erosion was observed by increasing the approach Froude number of the river after a hanging dam had already formed. Both the formation and erosion of the hanging dam were qualitatively compared with field observations of hanging dam occurrences using satellite imagery and hydrometric data to support the applicability of the experimental results to a field scenario. The results presented in this paper comprise the first published qualitative laboratory data on hanging dam formation, helping to improve our understanding of the fundamental mechanisms of hanging dam formation and evolution.

Keywords: hanging dam formation and evolution; physical modelling; incoming ice supply rate; approach Froude number; river ice engineering; ice transport; ice deposition

Citation: Senarathbandara, R.; Clark, S.P.; Dow, K. Experimental Analysis on Hanging Dam Formation and Evolution. *Water* **2023**, *15*, 4242. https://doi.org/10.3390/w15244242

Academic Editors: Spyros Beltaos and Brian C. Burrell

Received: 29 September 2023
Revised: 1 December 2023
Accepted: 8 December 2023
Published: 11 December 2023

1. Introduction

In a cold-region river, large quantities of frazil ice are generated in steep, fast flowing, open water river sections during the winter as a result of continuous supercooling and high turbulence [1]. The generated frazil ice particles are transported downstream and can become entrained underneath an existing downstream ice cover. The frazil ice entrained in the flow will either be transported as undercover ice or get deposited underneath the ice cover, depending on the hydraulic and geomorphic conditions of the river.

According to Ashton [2], the entrainment or the deposition of an ice floe at the leading edge of an ice cover is determined primarily based on the critical velocity and/or critical Froude number of the approach flow. MacLachlan [3] stated that the limiting velocity for ice deposition beneath an ice cover is 0.69 m/s and the ice cover may thicken if the flow velocity is lower than the critical velocity, which was based on data from the St. Lawrence River, Quebec, Canada. In the study on hanging ice dams by Kivisild [4], the critical Froude number of the approach flow was determined to be 0.08 for ice to become entrained beneath an ice cover, and the corresponding critical velocity was calculated as 0.61 m/s.

A thick frazil accumulation known as a hanging dam will form if there is a continuous frazil ice supply from upstream [5]. Hanging dams can be found at locations where there are significant decreases in the water velocity due to changes in the channel geometry, such as width expansions, depth increases, or channel slope reductions that promote ice deposition [6]. Depending on the size of the formation, hanging dams can have a substantial impact on the hydraulics of an ice-covered river. Channel bed scours can occur under a hanging dam due to the high flow velocity caused by the flow restrictions. In the Yellow River, China, near Hequ, a bed scour of 2 m was observed [7]. Hanging dam formation in a river can reduce the cross-sectional flow area, causing a flow restriction that may increase the flooding potential. Understanding the hanging dam formation process and quantifying the hanging dam evolution under various hydraulic and incoming ice supply conditions are important and may help address the flood risks that may be posed to communities near locations that are vulnerable to hanging dam formation. Minimizing hanging dam formation also enhances the hydraulic efficiency of hydropower generation.

It is often difficult to conduct field studies to monitor hanging dam formation due to the lack of accessibility to remote sites, safety conditions associated with potential ice cover failure, and cost considerations. Laboratory studies are an effective alternative to further understand the fundamental processes of hanging dam formation and evolution under various hydraulic and ice supply conditions with precise control of the hydraulic and geometric parameters.

The main objective of this study was to analyze the hanging dam formation under various hydraulic and incoming ice supply rate conditions using a laboratory physical model with a river issuing water into a relatively large reservoir with a simulated ice cover. Several parameters, such as the maximum length along the centreline, maximum thickness, location of maximum thickness, maximum width, and areal extent of the hanging dam, were quantified for various hydraulic and incoming ice supply rate conditions. The results of this study will improve the existing knowledge on hanging dam formation processes and its governing factors, and they will be beneficial to improve numerical modelling applications of hanging dam formation.

2. Background

Hanging dams are defined as thick accumulations of frazil ice beneath an existing ice cover [5]. Frazil ice particles generated in upstream, supercooled, turbulent, open water sections (following a 0 °C isotherm, where the water temperature drops below 0 °C) are transported downstream in the river and may become entrained beneath an existing ice cover. The entrained frazil ice will be transported as undercover ice and get deposited on the underside of the ice cover if the applied shear stress on the underside of the ice cover is insufficient to transport it further downstream [8]. The thickness of the accumulation will grow continuously to form a hanging dam unless the incoming frazil ice supply from upstream is limited/discontinued or the applied shear stress exceeds a limiting value. Previous field studies [5,9] show that an abrupt change in the geometry of a river that causes a reduction in the flow velocity, as well as the amount of the frazil ice supply from upstream, are two major contributing factors to hanging dam formation. The hanging dam formation process beneath a lake ice cover during the winter is illustrated in Figure 1 (adapted from [10]).

Several previous field studies report large hanging dam formations when the geometry of the river changes. In the winter of 1962, a field study was conducted at a hanging dam formation site in the Ottawa River. It was reported that there was a 75 m deep trench in the river with a width of 90 m that spanned over a length of 1.2 km. The flow velocity in the trench was considerably lower than the velocity of the river, which facilitated large depositions of frazil ice underneath the ice cover. The Long Sault Rapids are located immediately upstream of the hanging dam formation site. A large quantity of frazil ice was generated due to the high turbulence in the rapids and supercooled water temperature during the winter, which was transported in suspension to become deposited underneath the ice cover at the low-velocity downstream section. Two hanging dam formations with lengths of 450 m and 600 m and a width of 150 m were observed at this site [9].

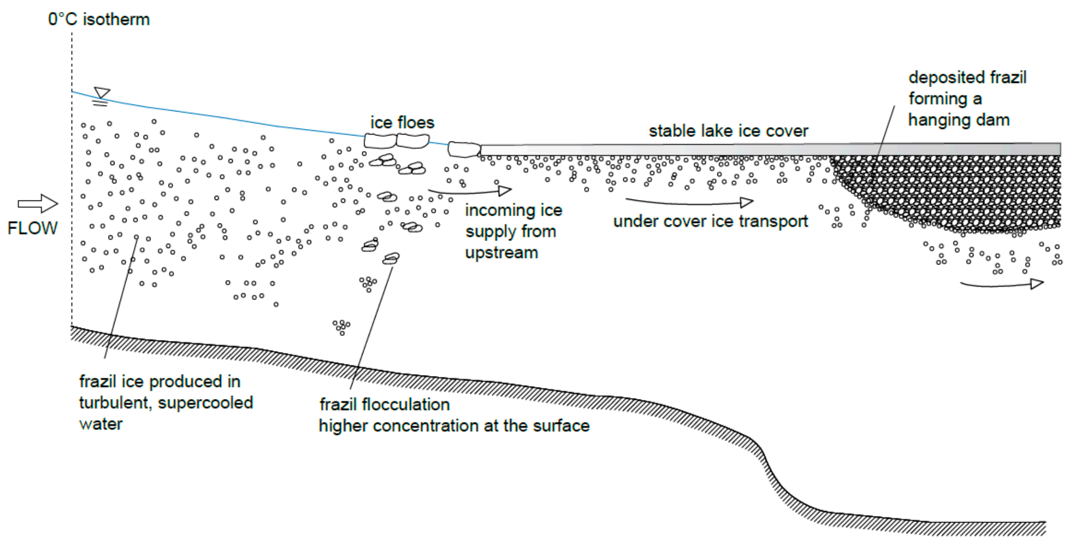

Figure 1. Hanging dam formation beneath a lake ice cover (adapted from [10]).

A hanging dam formation in the Smoky River, Alberta, was monitored in a series of field studies from 1975 to 1979. The field investigation showed that the length of the hanging dam formation varied from 300 m to 700 m and the maximum frazil accumulation thickness under the water surface varied from 11.0 m to 16.3 m during the study period. Similar to the Ottawa River hanging dam, this hanging dam was also located at a deep and wide section of the river immediately downstream of a rapids section. The non-submerged portion of the hanging dam (overburden) consisted of a layer of snow and weak granular ice. There was a 6 cm layer of thick solid ice on top of the overburden close to the riverbanks. The submerged portion comprised dense frazil slush with the pores saturated similar to those of the overburden, but with less cohesion. The frazil slush had a shape that varied between spheroid and discoid, with a diameter ranging from 1 to 6 mm. By weight, 60% of the frazil slush was in the range of from 1.1 mm to 2.4 mm in diameter, 35% was in the range of from 2.4 mm to 4.8 mm, and 5% was in the range of from 4.8 mm to 6.0 mm. The velocity underneath the hanging dam was measured using a magnetic flow meter, and the average velocity was reported as 0.12 m/s. Field tests were conducted to measure the shear strength and the bearing capacity using shear vanes from 1976 to 1979, and a scattered trend was obtained for both parameters. The authors suggested that this could be a result of the crudeness of the measuring technique and the natural variability in the shear strength [5].

Hanging dams can significantly impact the hydraulics of an ice-covered river by forming large accumulations that reduce the flow area, disrupt the flow, and even cause flooding. Each year, frazil ice accumulates in the St. Raymond reach of the St. Anne River, Quebec, in the form of grounded frazil jams or hanging dams. Even though flood-controlling structures were built to reduce the impacts from ice jam flooding, St. Raymond is repeatedly flooded during and after the break-up season each year. The study by Vergeynst, Morse, and Turcotte (2017) showed that 40% of the floods have occurred in the presence of ice in the river. The lack of knowledge on hanging dam formation processes and the river's ice regime were identified as the main reasons for the inability to successfully address the ice-related flooding issues in the St. Raymond reach, irrespective of the flood-controlling structures [11]. A comprehensive understanding of the processes leading to hanging dam formation and evolution will contribute to minimizing the flood risks posed to local communities near vulnerable locations.

Hopper and Raban (1980) investigated hanging dams in the Manitoba Hydro system and discussed their effects on river hydraulics and hydropower generation. The winter flows in the Burntwood River, Manitoba, increased from 20–34 m^3/s to 950 m^3/s as a result of the Lake Winnipeg Regulation and the diversion of the flow from the Churchill River to the Nelson River via the Burntwood River. It was predicted that a major hanging dam would form in the Burntwood River close to Thompson, Manitoba, causing high-river stages. After identifying this problem, a control structure and an ice boom were installed 6 km upstream from the potential hanging dam site to promote a stable ice cover and eliminate the ice-generating open water reach in the river. The authors concluded that this operation was successful and that the river stages were reduced by 8 m from the previous predicted levels [12].

The ice stabilization program in the Lake Winnipeg Regulation (LWR) was implemented in 1984 by cutting back flows at the Jenpeg control structure to facilitate ice cover formation in open water sections. During the operation, the cycling of the flow cutback was implemented such that the flows were decreased at night and increased during the day to minimize the effect of the flow cutback on the energy production [13]. The flow cutback procedure at the Jenpeg Generating Station decreased the discharge and the Froude number, which allowed the leading edge of the ice cover to progress over the rapids section, thereby decreasing the frazil ice production [14]. Through the ice stabilization program, Manitoba Hydro has successfully reduced the size of under-ice deposits in the reaches surrounding the Jenpeg Generating Station [13].

3. Methodology

Experiments were conducted in the hanging dam physical model shown in Figure 2, located at the Hydraulics Research and Testing Facility (HRTF) at the University of Manitoba. The physical model consisted of a narrow channel issuing into a much wider reservoir, hereafter referred to as the river and lake sections, respectively. The river section was 2.74 m long, 0.28 m in height, and had a width of either 0.16 m or 0.31 m to accommodate a range of approach Froude numbers. The lake section was 5.80 m long, 3.88 m wide, and 0.61 m in height. There was a difference in elevation of 0.31 m from the riverbed to the lakebed. The ratios of the lake width to the river width were 24 and 13 for river widths of 0.16 m and 0.31 m, respectively. The Dauphin River in Manitoba, Canada, enters Lake Winnipeg and a hanging dam forms at this confluence. In comparison, the ratio of the Dauphin River width to the width of the bay where the Dauphin River enters Lake Winnipeg was calculated as 17.

Water was pumped from a reservoir using either one or two pumps that had a combined capacity of 20 L/s. The flow was then conveyed to a headwater tank through a 0.1 m diameter pipe equipped with a paddlewheel flow meter. The upstream head water tank was 1.20 m wide, 1.20 m long, and 1.22 m in height and consisted of a flow straightener with an array of cylindrical pipes and a furnace filter to minimize the effects of turbulence on the flow. The outflow from the lake entered the downstream tailwater system via an opening at the downstream wall of the lake. A hopper system, as shown in Figure 3a, was installed to supply simulated ice upstream of the river section.

As shown in Figure 3c, high-density polyethylene (HDPE) pellets with a specific gravity of 0.95 and a nominal diameter of 3.1 mm were used as simulated frazil ice, and standard packing bubble wrap was used as a simulated ice cover. Initially, the flume was filled with water and the bubble wrap was set to cover the lake section (Figure 3b). Then, the pumps were set to achieve the discharge specified in the experimental conditions presented in Table 1. For each water discharge condition, simulated ice was supplied with two volumetric incoming ice supply rates of 0.0001 $m^3/s/m$ and 0.001 $m^3/s/m$ to observe the effect of the incoming ice supply rate on the hanging dam formation. For each experiment, the hanging dam was formed by supplying a total ice volume of 216 L from the hopper upstream of the river section. The time of the experiment varied according to the incoming ice supply rate. Ice was supplied for 72 min for an incoming supply rate of 0.0001 $m^3/s/m$, and for 18 min for an incoming supply rate of 0.001 $m^3/s/m$.

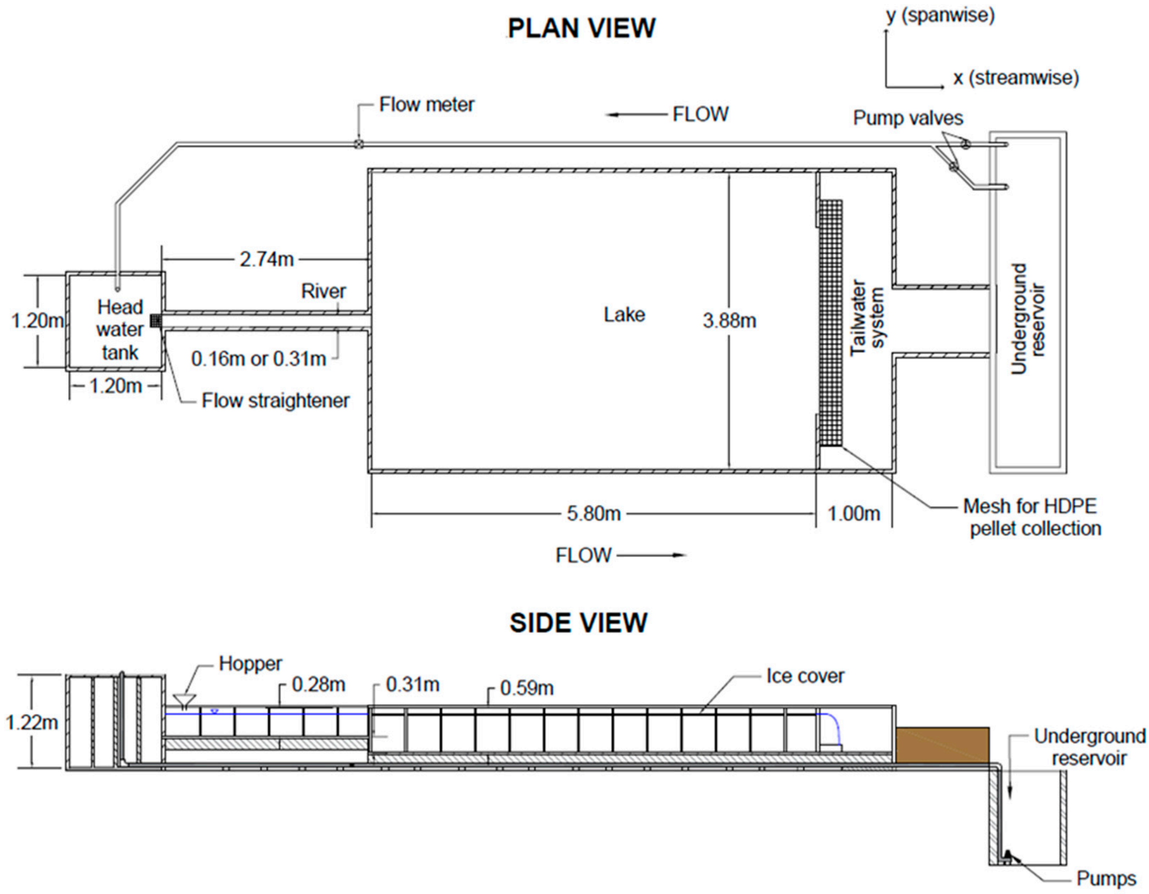

Figure 2. Schematic of the hanging dam experimental setup.

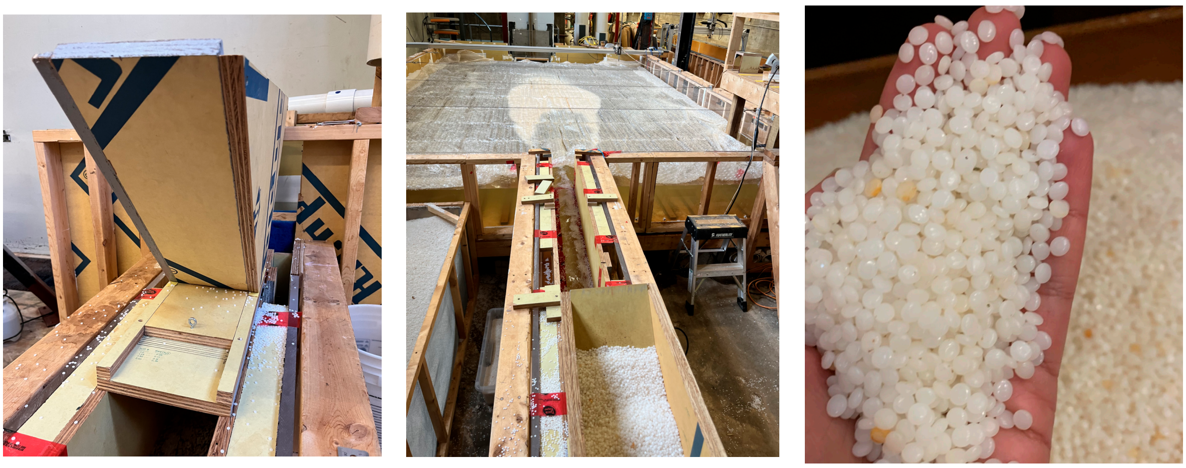

(**a**) (**b**) (**c**)

Figure 3. (**a**) Hopper system installed to supply pellets; (**b**) hanging dam experimental setup during an experiment; (**c**) HDPE pellets.

Table 1. Experimental conditions for hanging dam experiments.

Water Discharge (L/s)	Ice Discharge ($m^3/s/m$)	River Width (m)	River Depth (m)	Approach Velocity (m/s)	Approach Froude Number (-)	Lake Depth (m)
2.5	0.0001	0.31	0.057	0.14	0.19	0.38
2.5	0.001	0.31	0.057	0.14	0.19	0.38
4.0	0.0001	0.31	0.068	0.19	0.23	0.39
4.0	0.001	0.31	0.068	0.19	0.23	0.39
3.0	0.0001	0.16	0.063	0.30	0.38	0.38
3.0	0.001	0.16	0.063	0.30	0.38	0.38
4.2	0.0001	0.16	0.061	0.43	0.56	0.36
4.2	0.001	0.16	0.061	0.43	0.56	0.36
10.0	0.0001	0.16	0.095	0.66	0.69	0.37
10.0	0.001	0.16	0.095	0.66	0.69	0.37

The water depth in the river was measured using a point gauge, and the water depth in the lake was measured using a ruler attached to the lake wall. The average approach velocity (V) and the approach Froude number (Fr) in the river were calculated using Equation (1) and Equation (2), respectively, where Q is the water discharge (m^3/s), b is the river width (m), d is the water depth in the river (m), and g is the gravitational acceleration (m/s^2):

$$V = \frac{Q}{bd} \tag{1}$$

$$Fr = \frac{V}{\sqrt{gd}} \tag{2}$$

The aerial views of the hanging dam were captured using a GoPro Hero6 camera mounted to an overhanging wire above the hanging dam flume every 1 min during the ice supply. A Matlab package for georectifying oblique digital images developed by Bourgault et al. was used to orthorectify the aerial view images of the hanging dam [15]. The centreline length, maximum width, and areal extent of the hanging dam for each experiment were obtained from the orthorectified aerial view images. The image processing software ImageJ was used to measure the dimensions of the hanging dam formation [16], which were then divided by the lake depth to obtain dimensionless parameters.

Photogrammetry was used to obtain the maximum thicknesses of the hanging dam and their locations. To conduct the photogrammetry, water in the flume was slowly drained upon reaching a total ice supply volume of 216 L after the experiment, and the ice cover was carefully lifted off to the side. Four targets with known geometric coordinates with respect to the walls and the bed of the lake section were placed around the hanging dam. The photos of the hanging dam were taken using a Canon DSLR camera (Canon, Tokyo, Japan). The photos were imported to Agisoft Metashape photogrammetric processing software [17] to form an orthomosaic of the hanging dam. A digital elevation model (DEM) created using the orthomosaic was used to obtain the maximum thicknesses of the hanging dam and their locations. The detailed methodology of this procedure is discussed in [18].

4. Results and Discussion

4.1. Hanging Dam Formation

Figure 4 shows the orthorectified aerial views of the hanging dam for all approach Froude numbers and two incoming ice supply rates upon reaching the final ice volume of 216 L. The hanging dam formed immediately at or very close to the lake inlet for lower approach Froude numbers (Fr = 0.19 and 0.23), and the formation shifted further downstream as the approach Froude number increased. Flow from a narrow river into a lake is analogous to a three-dimensional wall jet, where the flow is directed along a wall to an ambient fluid. A wall jet is defined as a shear flow directed along a wall where the streamwise velocity over some region within the flow exceeds that in the external stream at any downstream location because of the initially supplied momentum [19]. The presence of a wall (ice cover) that directs the shear flow and the zero streamwise velocity at the wall (ice cover) due to the no-slip boundary condition are the primary similarities between a three-dimensional wall jet and the flow from a narrow river to a wide lake section. The high velocity of the wall jet for the approach Froude numbers 0.38, 0.56, and 0.69 did not allow under-ice deposition at the lake inlet, and the jet section can be seen in all these cases, where no ice was deposited immediately downstream of the river.

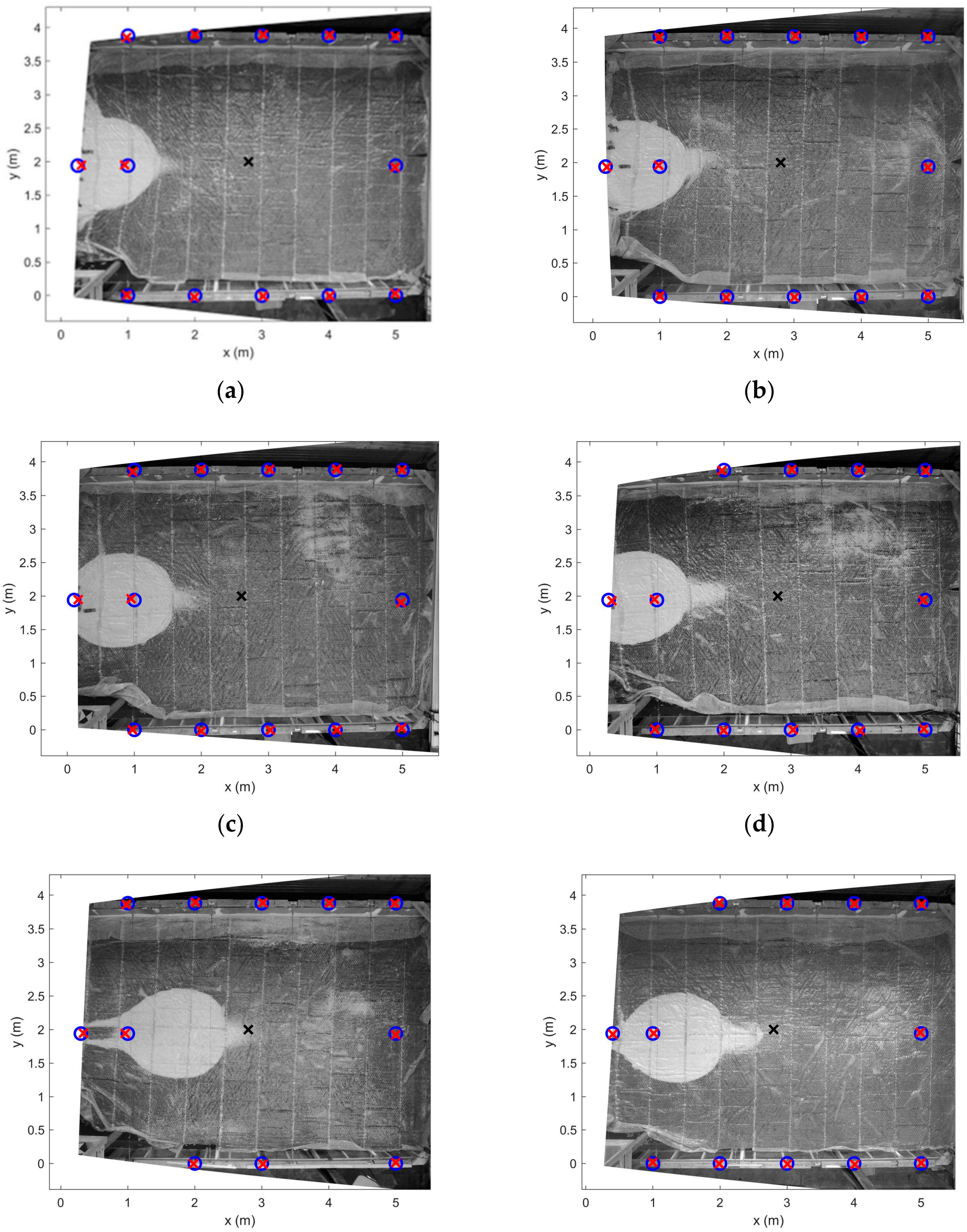

(**a**) (**b**) (**c**) (**d**) (**e**) (**f**)

Figure 4. *Cont.*

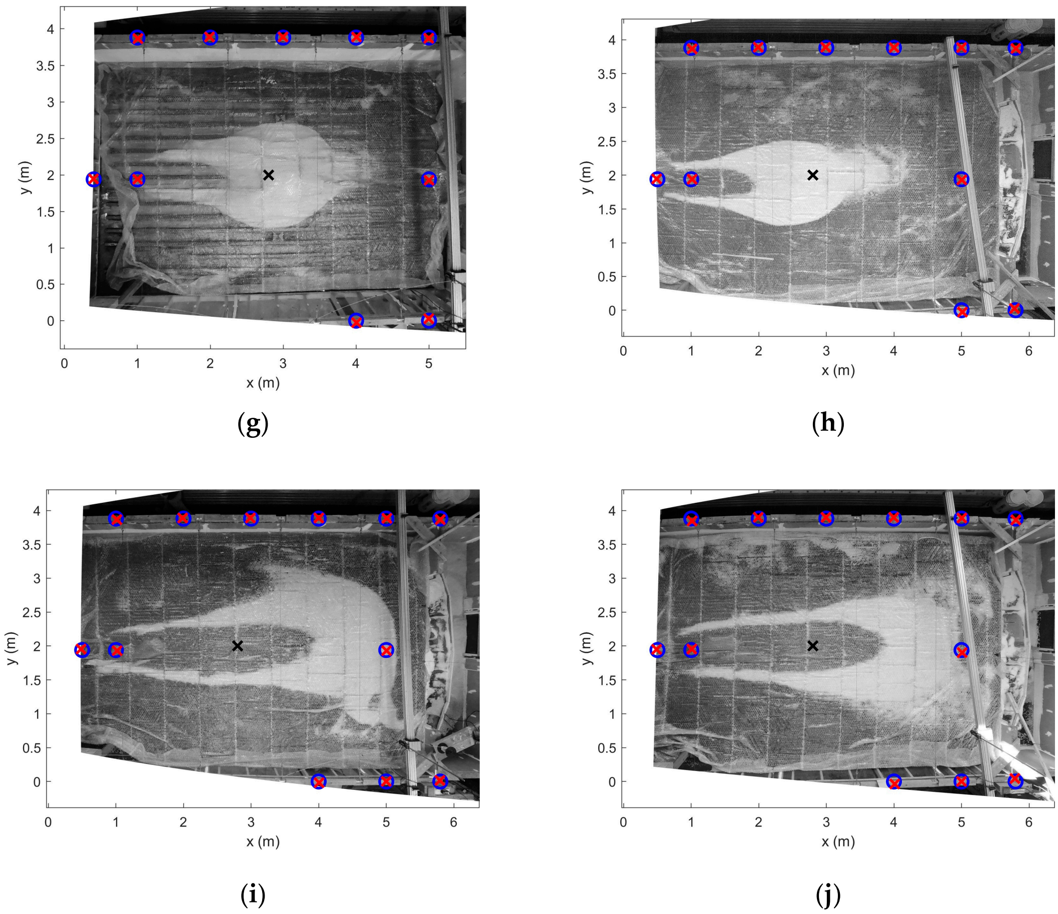

Figure 4. Aerial views of hanging dam formation for various Froude numbers and incoming ice supply rates: (**a**) Fr = 0.19, q_i = 0.0001 $m^3/s/m$; (**b**) Fr = 0.19, q_i = 0.001 $m^3/s/m$; (**c**) Fr = 0.23, q_i = 0.0001 $m^3/s/m$; (**d**) Fr = 0.23, q_i = 0.001 $m^3/s/m$; (**e**) Fr = 0.38, q_i = 0.0001 $m^3/s/m$; (**f**) Fr = 0.38, q_i = 0.001 $m^3/s/m$; (**g**) Fr = 0.56, q_i = 0.0001 $m^3/s/m$; (**h**) Fr = 0.56, q_i = 0.001 $m^3/s/m$; (**i**) Fr = 0.69, q_i = 0.0001 $m^3/s/m$; (**j**) Fr = 0.69, q_i = 0.001 $m^3/s/m$ (flow direction: from left to right; white area: hanging dam extent; pink markers: ground control points; black cross marker: camera location).

The spatial evolution of the hanging dam in terms of the maximum length along the centreline and the maximum width was analyzed for the three lowest Froude numbers (Fr = 0.19, 0.23, and 0.38), as the approach Froude number of an ice-covered river during the winter is typically of a low value. Figure 5 shows the evolution of the dimensionless maximum centreline length (maximum centreline length/lake depth) of the hanging dam for various approach Froude numbers for the two incoming ice supply rates. Initially there was a rapid increase in the centreline length, but the length plateaued and approached a constant value when the t/t_{final} was approximately 0.2, where t is the time at a specific moment and t_{final} is the time taken to reach an ice supply volume of 216 L. This can be explained based on the momentum supplied by the velocity of the jet. Initially, the incoming ice supply to the flume is transported along the flow of the jet and deposited beneath the ice cover when the velocity is not adequate to transport the ice further downstream. The subsequent ice supply to the flume is deposited in the area in between the initially reached centreline length and the lake inlet, increasing the thickness of the accumulation. The final centreline length of the hanging dam has a direct relationship with the approach Froude number of the flow, where the centreline length increases when the approach Froude number increases, as ice is transported further downstream due to the high velocity of the jet at high approach Froude numbers.

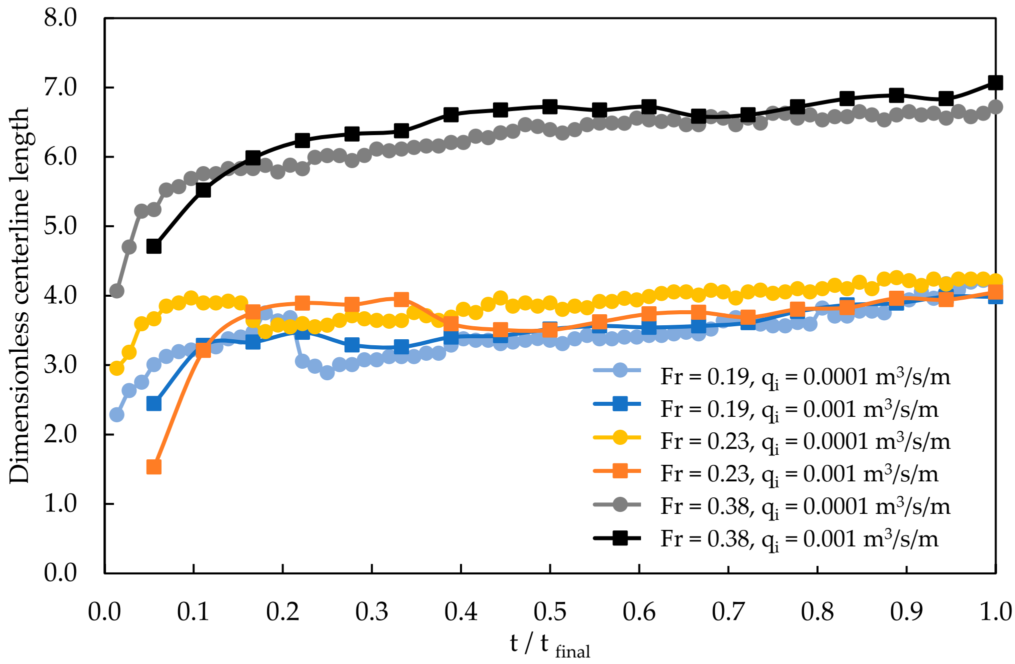

Figure 5. Evolution of dimensionless centreline length (centreline length/lake depth) for various approach Froude numbers.

The spatial evolution of the dimensionless maximum width (maximum width/lake depth) of the hanging dam is shown in Figure 6. For all the cases, the maximum width of the hanging dam increased as more ice was supplied to the flume. Irrespective of the Froude number and incoming ice supply rate, the dimensionless maximum width of the hanging dam reached a constant value upon reaching the final volume of the hanging dam. Even though it is not possible to produce a similar plot for the evolution of the maximum thickness of the hanging dam, it would have increased with the increasing ice supply in a trend similar to that of the maximum width.

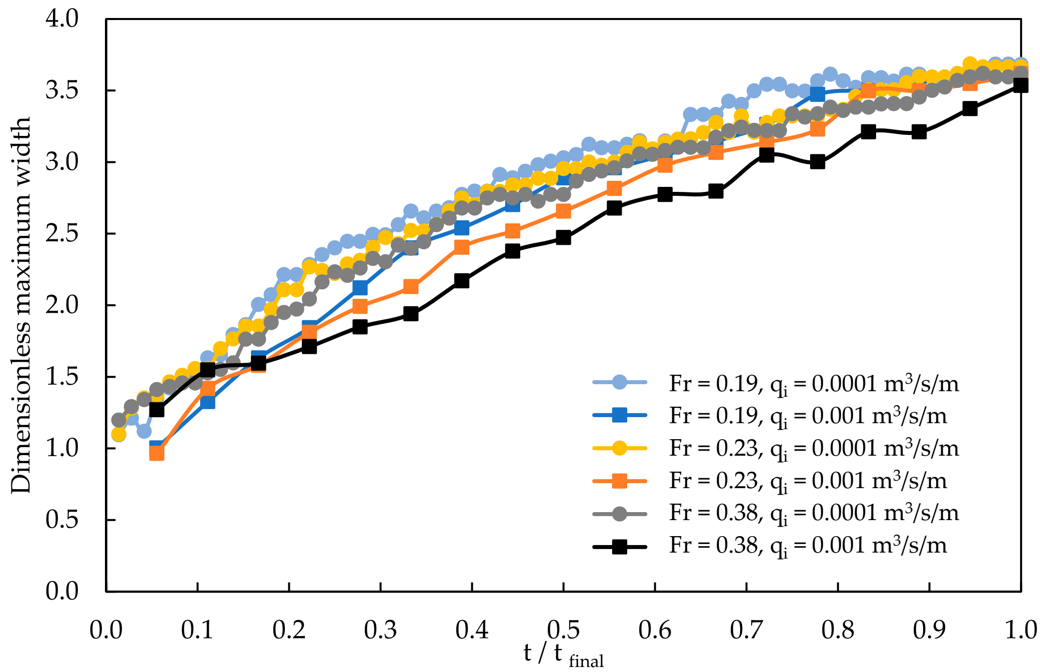

Figure 6. Evolution of dimensionless maximum width (maximum width/lake depth) for various approach Froude numbers.

The final longitudinal profiles of the hanging dams obtained from photogrammetry at the centreline of the lake section for various Froude numbers are shown in Figure 7. For the lowest-Froude number (Fr = 0.19) experiment, the hanging dam formed immediately at the lake inlet for both high and low incoming ice supply rates. The hanging dam formed immediately at the lake inlet only at the high incoming supply rate for the Froude number 0.23. As the Froude number increased, the hanging dam formed further downstream due to the high shear stress exerted by the flow of the jet. For all the approach Froude numbers, the maximum thickness of the hanging dam occurred closer to the lake inlet at the higher incoming ice supply rate when compared with the low incoming ice supply rate.

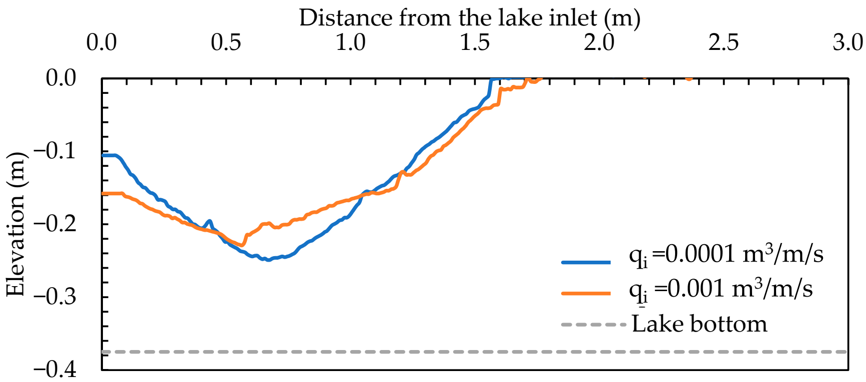

(**a**)

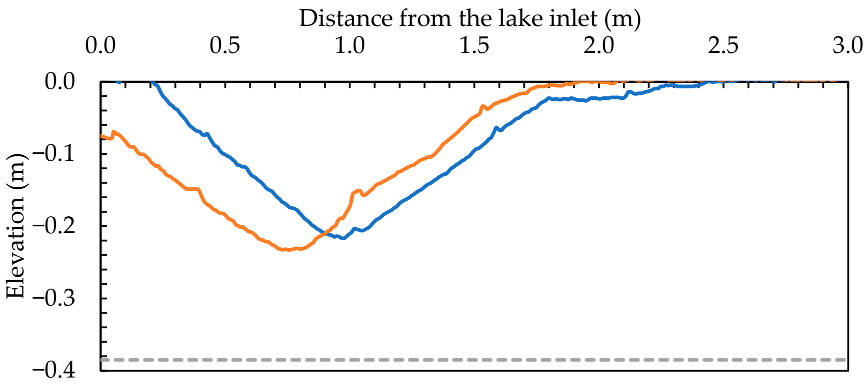

(**b**)

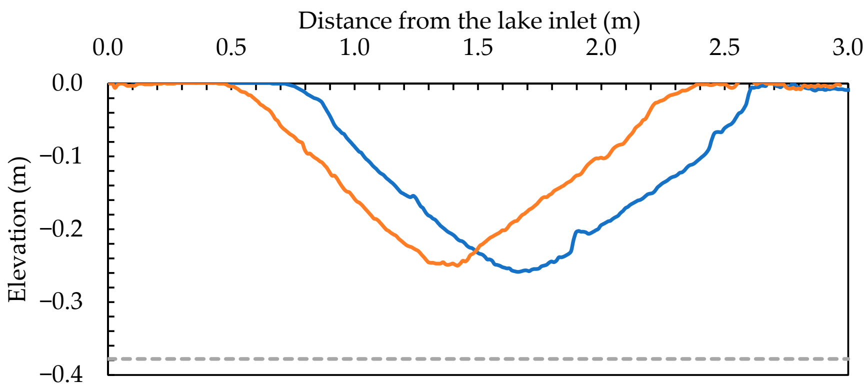

(**c**)

Figure 7. *Cont.*

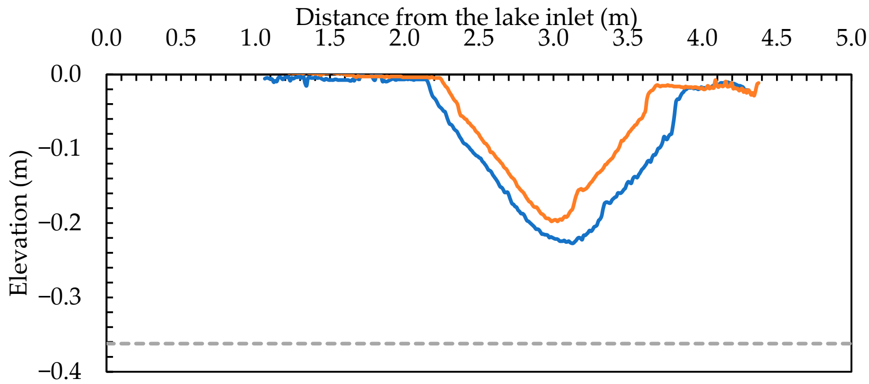

(**d**)

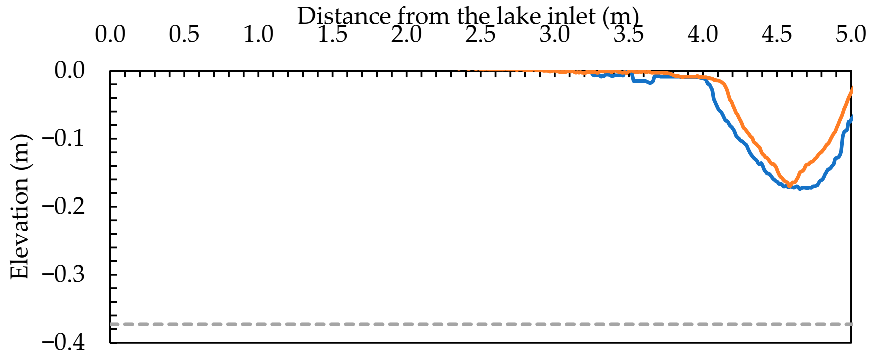

(**e**)

Figure 7. Longitudinal profiles of the hanging dam at the centreline of the lake section for various Froude numbers: (**a**) Fr = 0.19; (**b**) Fr = 0.23; (**c**) Fr = 0.38; (**d**) Fr = 0.56; (**e**) Fr = 0.69.

The maximum thicknesses of the hanging dam formation (T_{max}) for the two incoming ice supply rates and various approach Froude numbers are shown in Figure 8. The highest thickness was observed at an approach Froude number of 0.38. The maximum thicknesses for the approach Froude numbers of 0.19 and 0.23 were just slightly lower than the maximum thickness at a Froude number of 0.38. For the low-Froude-number conditions, the maximum dimensionless thickness of the hanging dam plateaued around a dimensionless length of 0.68, which corresponds to a thickness of 0.25 m. The growth of the thickness of the hanging dam was hindered by several factors, such as the fixed lakebed that only allowed a flow depth of 0.12 m during the thick hanging dam formation, and the absence of cohesion due to freezing. Figure 9 shows the side view of the hanging dam formation at the lake inlet for an approach Froude number of 0.19 after reaching the maximum thickness of 0.25 m. The maximum thickness of the hanging dam decreased with increasing approach Froude numbers because the velocity of the jet was high at higher Froude numbers and the hanging dam accumulation was pushed further downstream in the lake section. At a specific approach Froude number, the maximum thicknesses of the hanging dam reached similar values irrespective of the incoming ice supply rate. The maximum thickness of the hanging dam was governed by the fixed lakebed and the absence of cohesion in the HDPE pellets. The shear stress on the underside of the accumulation increases as the hanging dam grows in thickness and non-cohesive pellets easily erode due to this high shear stress. On the contrary, a hanging dam in a natural environment could reach extremely high thicknesses as long as there is a sufficient water depth such that the applied shear stress underneath the hanging dam is lower than the critical shear stress that initiates erosion. During the initial ice formation stages, the thermal effects of ice play an important role in forming an ice cover near the water surface. The thermal ice cover can grow in thickness, which may also contribute to a portion of the hanging dam, which was not simulated in this laboratory study.

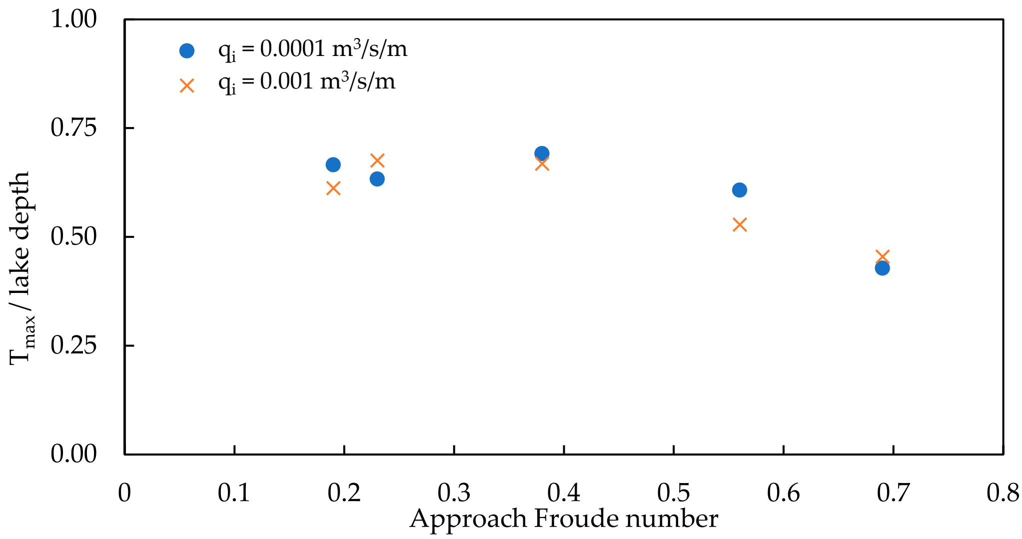

Figure 8. Maximum thicknesses of the hanging dam for various approach Froude numbers and incoming ice supply rates.

Figure 9. Side view of the hanging dam at the lake inlet for an approach Froude number of 0.19.

The locations of the maximum thicknesses of the hanging dam (L_{max}) for various approach Froude numbers and the two incoming ice supply rates are shown in Figure 10. The maximum thicknesses of the hanging dam occurred further downstream as the approach Froude number increased due to the high-velocity jet coming out of the river that pushed the formation downstream. The maximum thicknesses for lower incoming ice supply rates were located further downstream when compared with the locations of the higher supply rates for the same Froude number. During the ice supply stage of hanging dam formation, both deposition and erosion processes happen at the same time at different locations, making the process quite dynamic. Erosion is facilitated through the shear force exerted by the jet flow, and if the incoming ice supply from upstream is not adequate to maintain the rate of erosion, the subsequent depositions happen further downstream.

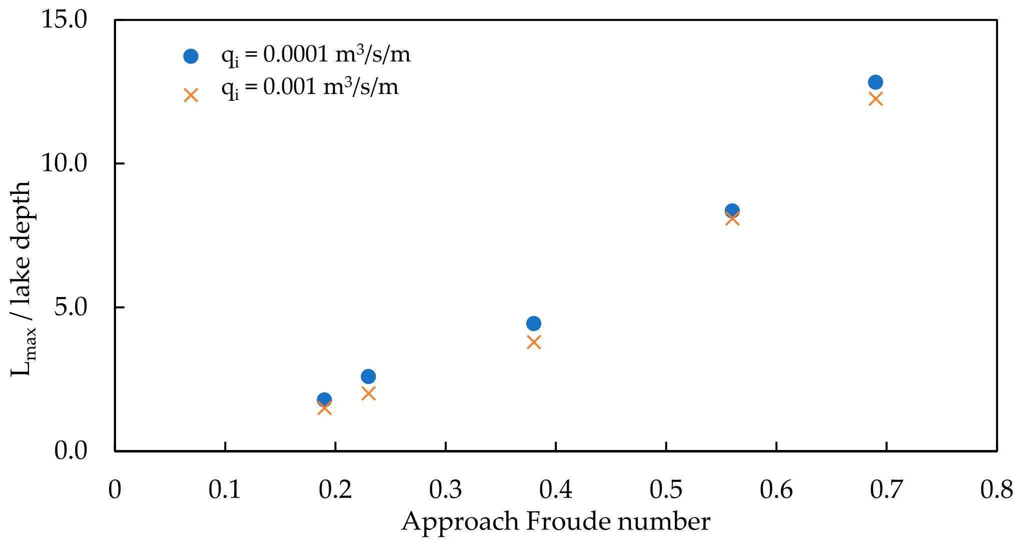

Figure 10. Locations of maximum thicknesses of the hanging dam for various approach Froude numbers and incoming ice supply rates.

The areal extents of the hanging dam (A_{max}) for various approach Froude numbers and two incoming ice supply rates are shown in Figure 11. The areal extent of the hanging dam increased with increasing Froude numbers, and the areal extent for the lower incoming ice supply rate experiment was higher than that of the high ice supply rate experiment for the same approach Froude number. At a low ice supply rate, the rate of supply was not adequate to overcome the rate of erosion; therefore, the eroded ice was transported in both the streamwise and spanwise directions and became deposited at a location further away from the high erosive power of the jet. This also means that if the incoming ice supply from upstream is abruptly terminated and the water discharge is maintained the same, the hanging dam will evolve with erosion and finally reach a stable state. An erosion experiment was conducted to further investigate this theory.

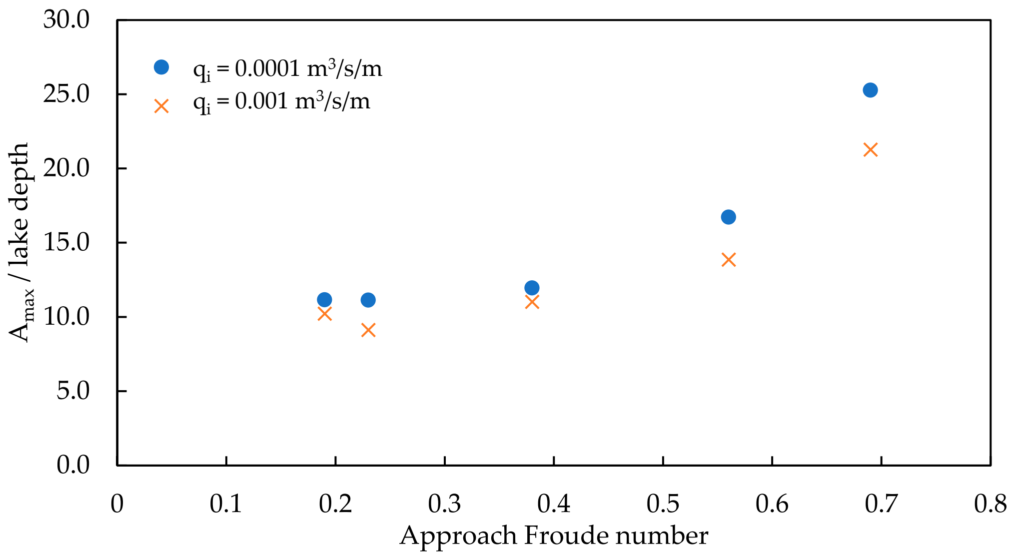

Figure 11. Areal extents of the hanging dam for various approach Froude numbers and incoming ice supply rates.

4.2. Hanging Dam Erosion

For the erosion experiment, a hanging dam was formed with a volumetric incoming ice supply rate of 0.0001 $m^3/s/m$ and an approach Froude number of 0.19. Ice was supplied to the flow until a total ice volume of 216 L was reached. Figure 12a shows the hanging dam formation immediately after finishing the ice supply. The water discharge was incremented in two steps, as specified in Table 2, until erosion was observed, and an aerial photo was taken using a GoPro camera every minute to observe the erosion process.

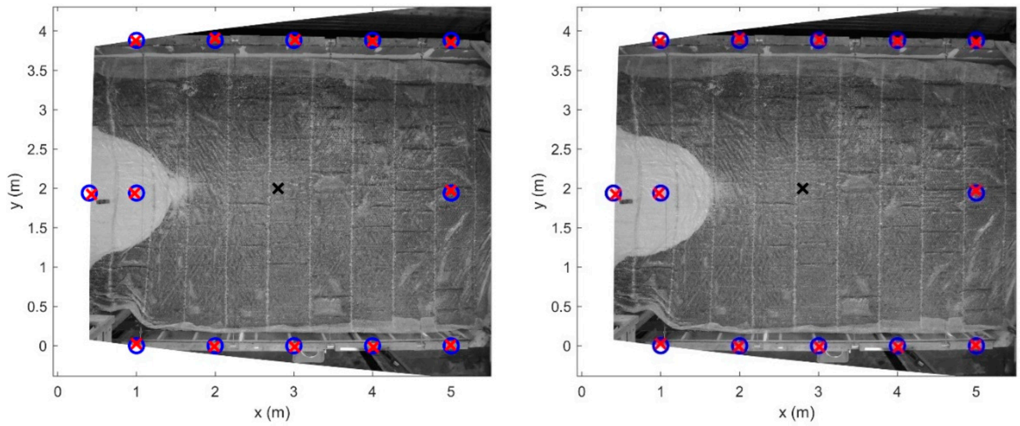

(**a**) (**b**)

Figure 12. Aerial views of the hanging dam (**a**) immediately after terminating the ice supply and (**b**) 15 min after setting an approach Froude number of 0.25 (flow direction: from left to right; white area: hanging dam extent; pink markers: ground control points; black cross marker: camera location).

Table 2. Experimental conditions for hanging dam erosion experiments.

Condition	Water Discharge (L/s)	Approach Froude Number (-)	Approach Velocity (m/s)
Formation	2.5	0.19	0.14
First step for erosion	4.6	0.25	0.21
Second step for erosion	7.9	0.33	0.30

As the first step, the discharge was set to 4.6 L/s with an approach Froude number of 0.25. Figure 12b shows the aerial view of the hanging dam after 15 min with the first flow condition; only a modest amount of erosion can be inferred from the slightly larger aerial extent of the hanging dam. The discharge was increased to 7.9 L/s with an approach Froude number of 0.33, and the hanging dam started to erode noticeably. Figure 13a–d show the aerial views of the hanging dam at 5, 15, 25, and 35 min after setting the second discharge condition. The total centreline length and the open water jet length were measured from the aerial view images and plotted against time, as shown in Figure 14. Initially, the total centreline length of the hanging dam increased due to erosion; however, the rate of change in the total centreline length was reduced 15 min after setting the discharge. The rate of change in the open-water jet length also dropped and reached a steady state approximately 25 min after setting the discharge. The erosion of the hanging dam formation was caused by the shear stress exerted on the underside of the ice cover from the jet flow. The wall jet theory explains that the streamwise velocity in the region close to the jet initiation (lake inlet) is higher than the streamwise velocity at any downstream location because of the initially supplied momentum. At the start of the erosion process, the ice deposited close to the lake inlet is transported further downstream based on the shear stress supplied by the flow of the jet and is deposited in an area where the velocity is very low or negligible. The outline of the wall jet can be seen in the aerial view photos as an open-water section.

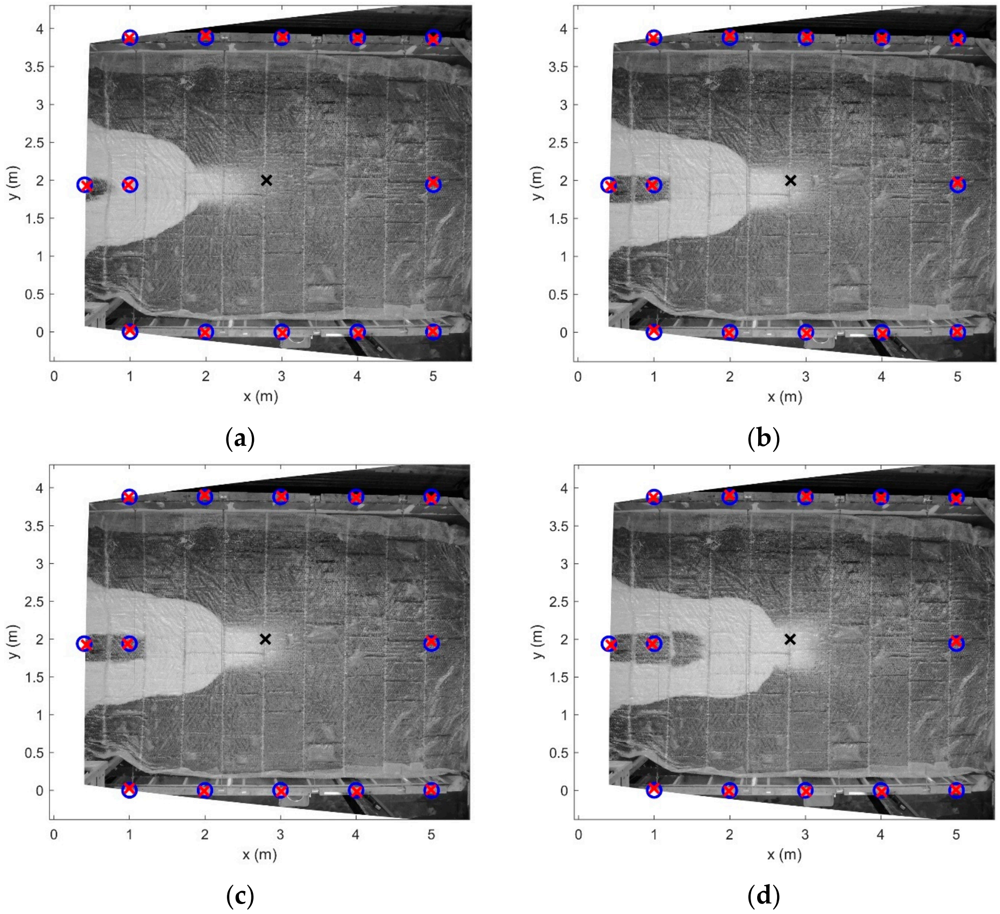

Figure 13. Aerial views of hanging dam erosion (**a**) 5 min, (**b**) 15 min, (**c**) 25 min, and (**d**) 35 min after stopping the ice supply (flow direction: from left to right; white area: hanging dam extent; pink markers: ground control points; black cross marker: camera location).

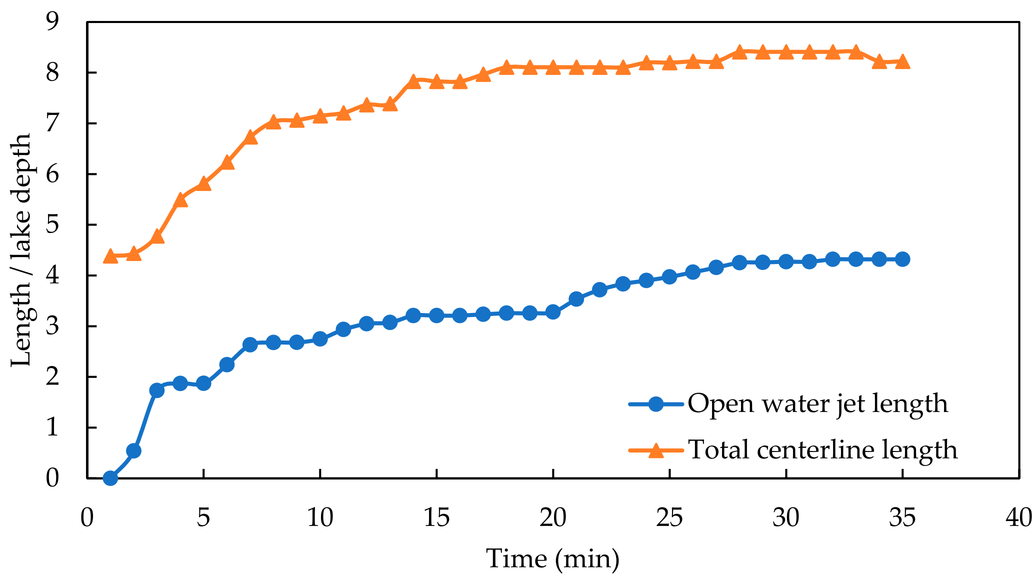

Figure 14. Evolution of the total centreline length and open-water jet length of the hanging dam during erosion.

4.3. Comparison to Field Data

The experimental results were qualitatively compared with two hanging dam occurrences in the field using optical imagery from satellites and hydrometric data. The first case was the hanging dam formation at the confluence of the Dauphin River and Lake Winnipeg in central Manitoba. The Dauphin River is about 52 km long and drains into Lake Winnipeg. Based on the difference in the channel slope, this river can be classified into two reaches: an upper reach with a slope of 0.029% over 40 km and a lower reach with a slope of 0.16% over 11.2 km. The steep lower reach of the river has open-water areas with velocities that exceed 1.5 m/s and can generate a significant volume of frazil ice during the freeze-up season [20]. A hanging dam forms at the outlet to Lake Winnipeg when the frazil ice is deposited under the lake ice cover [21]. The ice-affected water levels in the steep lower reach can rise 4–5 m or more above those of the open-water conditions due to thick ice jams [22].

The shape and areal extent of the hanging dam were visible from satellite images when the lake ice cover was relatively thin, typically at the end of the winter during the months of April and May. Optical imagery was obtained from Landsat 8/9 and Sentinnel-2 satellites from the US Geological Survey's EarthExplorer [23,24] for days with low cloud coverage.

An HEC-RAS model of the Dauphin River [22] was used to estimate the Froude number at the most downstream cross section of the river. The mean monthly discharge and the mean monthly water level at the Dauphin River Water Survey of Canada gauge (05LM006) were used as the upstream and downstream boundary conditions for the HEC-RAS model, respectively. The model was set to run in a steady state for each month during the ice-affected period (from November to April), and the Froude number at the downstream cross section of the river was obtained. The average ice-affected Froude number for 2017–2018 was estimated as 0.06 from HEC-RAS model simulations.

The ice discharge in a river is correlated to the air temperature. A field estimation of the incoming ice discharge in the Dauphin River was previously conducted using an analysis of unmanned aerial vehicle (UAV) videos taken at a site 25 km upstream of the lake inlet for the 2017–2018 season. The ice discharge was calculated using Equation (3), where Q_{ice} is the ice discharge (m^3/s), V_{ice} is the average surface ice velocity (m/s), N is the average surface ice concentration (-), B is the river width (m), and t_{ice} is the average thickness of a surface ice floe (m):

$$Q_{ice} = V_{ice} N B t_{ice} \tag{3}$$

The average thickness of the ice floes was considered a major unknown when using this method and was estimated to vary between 0.05 m and 0.15 m according to field measurements. The ice discharge in the river for the 2017–2018 season was calculated to vary between 1.1 m^3/s and 3.4 m^3/s [22]. The corresponding volumetric incoming ice discharge (q_i) at the lake inlet was calculated to vary between 0.004 $m^3/s/m$ and 0.01 $m^3/s/m$ using Equation (4), where the width of the river immediately upstream of the lake inlet was determined to be 120 m using the bathymetry data:

$$q_i = \frac{Q_{ice}}{B} \tag{4}$$

Figure 15a shows the hanging dam formation at the Dauphin River–Lake Winnipeg confluence for the 2017–2018 season, where the average approach Froude number is equal to 0.06. This case from the field can be compared with the lowest Froude number experiment shown in Figure 15b, where the approach Froude number was 0.19 and the incoming ice supply rate was 0.001 $m^3/s/m$. In both cases, ice deposition occurred immediately at the lake inlet, where the flow velocity was reduced due to the abrupt increase in the channel width and depth. Ice was deposited in a semi-circular shape around the inlet of Lake Winnipeg, similar to the experimental case, suggesting that there was a high incoming ice supply during the formation stage of this hanging dam. In comparison, the ratio of the lake width (at the bay where the Dauphin River enters Lake Winnipeg) to the Dauphin River width was 17, whereas the physical model had a lake width–river width ratio of 13. The field observations and analysis by Wazney [22] indicated that the ice discharge in the Dauphin River was as high as 3.4 m^3/s, based on the thickness of the ice floes, during the 2017–2018 freeze-up season.

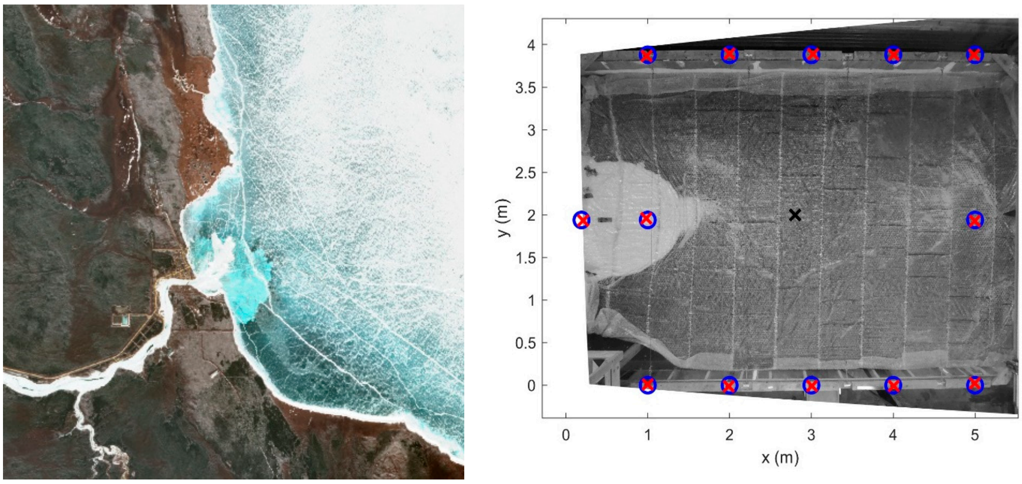

(**a**) (**b**)

Figure 15. Hanging dam formation (**a**) at Dauphin River–Lake Winnipeg confluence on 21 April 2018 (image courtesy of the USGS) and (**b**) for the experiment with an approach Froude number of 0.19, qi = 0.001 $m^3/s/m$ (flow direction: from left to right; white area: hanging dam extent; pink markers: ground control points; black cross marker: camera location).

Figure 16a shows the hanging dam on 3 May 2018 during the breakup season. The higher river discharge and warmer water temperature seem to have caused the hanging dam to have eroded (either mechanically, thermally, or likely a combination of both) along a preferential path. Figure 16b shows the aerial view of the hanging dam 35 min after setting an approach Froude number of 0.33 during the erosion experiment, where the erosion was caused by the higher river discharge. In both cases, the open-water jet section that results from the higher river discharge is clearly visible. The thermal effect on erosion is an important difference between a field study and a laboratory study. In the Dauphin River field study, rising air temperatures might have contributed to the erosion of the hanging dam, whereas the erosion in the experiments was caused entirely by the flow of the jet.

Another hanging dam can be found downstream of the Keeyask Generating Station on the lower Nelson River, Manitoba. The Keeyask Generating Station is located between the outlet of Split Lake and the inlet to Stephens Lake, with average winter flows of 3300 m^3/s. The lower Nelson River is a complex, fast-flowing hydraulic system that contains reaches that are separated by rock controls, rapids, and lakes. The ice processes in this river are complex due to the presence of rapids that produce a large quantity of frazil ice during the winter and the interconnected system of river reaches and lakes. During the winter, a large hanging dam forms at the inlet to Stephens Lake that is located immediately downstream of the Gull Rapids. There is a 13 m drop in elevation from Gull Lake to Stephens Lake, and the majority of the drop spans across the Gull Rapids.

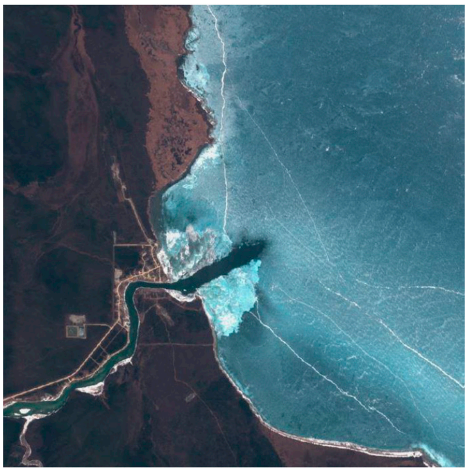

(**a**)

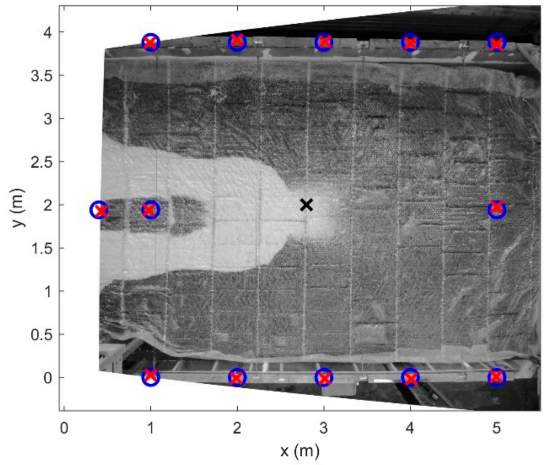

(**b**)

Figure 16. Hanging dam erosion (**a**) at Dauphin River–Lake Winnipeg confluence on 3 May 2018 (image courtesy of the USGS) and (**b**) for the experiment with an approach Froude number of 0.33(flow direction: from left to right; white area: hanging dam extent; pink markers: ground control points; black cross marker: camera location).

The lake ice cover on Stephens Lake forms in early fall, causing the frazil ice generated in the Gull Rapids to collect at the leading edge of the ice cover. The ice cover progresses upstream until reaching the rapids section downstream of the Keeyask Generating Station, where it stalls. The incoming frazil ice from upstream is deposited beneath the ice cover forming a hanging dam at this location. This hanging dam initially grows very rapidly, but the growth rate slows down later depending on whether an ice bridge forms upstream of Gull Lake. The frazil ice supply from upstream is reduced substantially if the ice cover bridges upstream of Gull Lake, which impacts the size of the hanging dam formation [25].

The size and the location of the hanging dam at this site can be seen in satellite imagery when the lake ice cover is thin, typically in mid-May. Satellite images of the hanging dam from Sentinel-2 and Landsat 8/9 satellites were obtained from the US Geological Survey's EarthExplorer [23,24] for a period of 10 years from 2013 to 2023. The hanging dam was not visible in some years due to high cloud coverage. Figure 17 shows the hanging dam downstream of the Keeyask Generating Station in 2013 and 2023. The areal extent of the hanging dam has decreased over the years, and a significant difference in the areal extent can be observed when comparing the formation of 2013 with that of 2023.

The Keeyask Generating Station started operations in March 2022, which is the main difference between the 2012–2013 and 2022–2023 seasons. The ice boom installed at Gull Lake and the flow control procedures taken by the generating station as part of their operations may have ensured the formation of a competent ice cover upstream of the rapids section, lowering the frazil ice production. There are open water sections visible in the 2013 satellite image upstream of the hanging dam location, but these sections are ice-covered in the 2023 satellite image.

The mean daily air temperatures at Gillam Airport (the closest meteorological site to the Keeyask Generating Station) were analyzed for the two winter seasons (October–May) for 2012–2013 and 2022–2023. The cumulative degree days of freezing (CDDF) for the 2012–2013 winter were calculated as 3323, while the 2022–2023 winter had 3065 cumulative degree days of freezing, indicating that the 2022–2023 winter was warmer than the 2012–2013 winter.

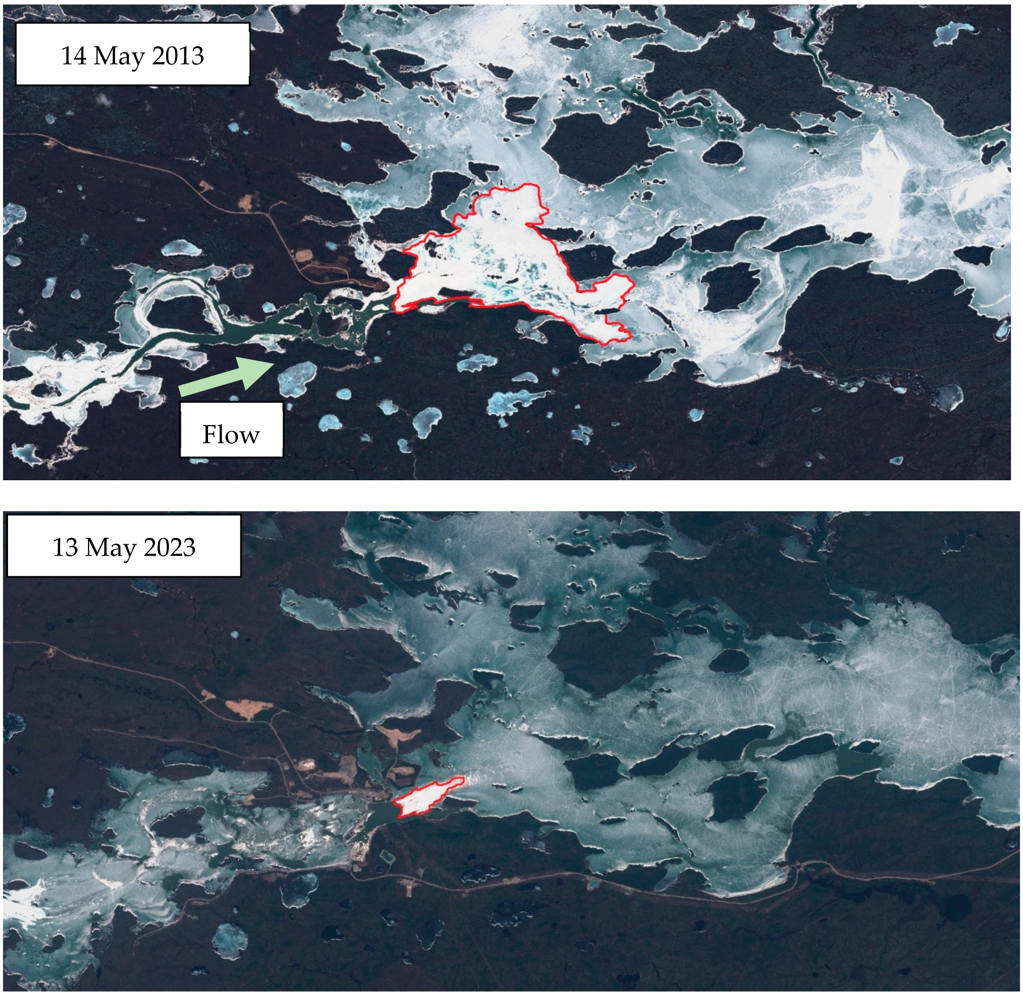

Figure 17. Hanging dam formation downstream of Keeyask Generating Station in 2013 and 2023 (the extent of the hanging dam is outlined in red).

The results presented in this paper comprise the first published qualitative laboratory data on hanging dam formation, but there are several limitations of this study that need to be highlighted. The thermal effects on the hanging dam formation were not taken into consideration, as it is practically difficult to incorporate the thermal component in a laboratory environment. Frazil ice is cohesive and easily freezes together, unlike the HDPE pellets that were used as simulated ice in this laboratory study. In a natural river, hanging dams can attain extremely high thicknesses if the applied shear stress beneath them is less than the critical shear stress that initiates erosion. In this laboratory study, the flow depth was limited; therefore, the maximum thicknesses of the hanging dam reached similar values for all the different ice supply rate conditions.

The under-ice roughness, shear stress, and velocity change as the accumulation increases in thickness. Quantifying these parameters would be beneficial when validating numerical models as well as provide an additional insight when making comparisons with field data. An acoustic Doppler velocimeter (ADV) was considered to obtain the velocity measurements in this study, but it could not be used during the ice supply stage because the ADV probe disturbed the hanging dam formation. The use of an alternative technique to measure the velocity beneath the hanging dam is suggested for future studies, as it will be a valuable addition to the existing hanging dam literature.

5. Conclusions

The effects of the approach Froude number of a river and the incoming ice supply rate on the hanging dam formation and evolution processes were analyzed in this study. Hanging dam erosion that is enabled by a higher river discharge (at a higher approach Froude number) was also discussed. The results of this study were obtained from a series of laboratory experiments in a hanging dam physical model using HDPE pellets and bubble wrap as the simulated frazil ice and simulated ice cover, respectively.

The hanging dam formed immediately at or very close to the lake inlet at lower approach Froude numbers when compared with higher approach Froude numbers, as the high velocity of the three-dimensional wall jet did not allow under-ice deposition at the lake inlet at higher Froude numbers. The maximum centreline length of the hanging dam increased with increasing Froude numbers, but the maximum width was not dependent on either the Froude number or the incoming ice supply rate. The maximum width of the hanging dam reached a constant value for all low-approach-Froude-number experiments at the final volume of the hanging dam.

The maximum thickness decreased and the location of the maximum thickness was further downstream with increasing approach Froude numbers due to the high velocity of the jet that pushes the hanging dam formation further downstream at high approach Froude numbers. The areal extent of the hanging dam increased with increasing Froude numbers. The low-incoming-ice-supply-rate experiments had higher areal extents compared to the high-incoming-ice-supply-rate experiments for the same Froude number, as the low incoming ice supply rate was not adequate to overcome the under-ice erosion rate exerted by the flow of the jet.

The satellite imagery of the hanging dam at the Dauphin River–Lake Winnipeg confluence was compared to the laboratory experiments to note the similarities in the formation and erosion of the hanging dam. Decades-apart satellite images (2013 and 2023) of the hanging dam downstream of the Keeyask Generating Station were compared, and a considerable reduction in the areal extent of the hanging dam was noticed. The possible effects of the flow control procedures implemented by the generating station as a part of their operations and the milder winter were noted to be the primary reasons for the reduction in the hanging dam size.

This is the first study of its kind that presents the relationship between the approach Froude number and the incoming ice supply rate on hanging dam formation and evolution, contributing to improving our understanding of these processes. The wall jet comparison to hanging dam formation is of interest for numerical modelling applications simulating hanging dam formation and evolution.

Author Contributions: Conceptualization, R.S.; methodology, R.S.; validation, R.S.; formal analysis, R.S.; investigation, R.S.; resources, S.P.C. and K.D.; writing—original draft, R.S.; writing—review and editing, S.P.C. and K.D.; visualization, R.S.; supervision, S.P.C. and K.D.; funding acquisition, S.P.C. and K.D. All authors have read and agreed to the published version of the manuscript.

Funding: This research was funded by the Manitoba Hydro and the Natural Sciences and Engineering Research Council of Canada, grant number CRDPJ 543865-19.

Data Availability Statement: Data are available upon request from the authors.

Acknowledgments: The authors would like to thank Alexander Wall for his assistance with the experimental setup, and Danica Bodino for orthorectifying the aerial view images.

Conflicts of Interest: The authors declare no conflict of interest. The funders had no role in the design of the study; in the collection, analyses, or interpretation of the data; in the writing of the manuscript; or in the decision to publish the results.

References

1. Hicks, F. An overview of river ice problems: CRIPE07 guest editorial. *Cold Reg. Sci. Technol.* **2009**, *55*, 175–185. [CrossRef]
2. Ashton, G.D. Froude criterion for ice block stability. *J. Glaciol.* **1974**, *13*, 307–313. [CrossRef]
3. MacLachlan, D.W. Appendix E. In *St. Lawrence Waterways Project Report*; Joint Board of Engineers: Ottawa, ON, Canada, 1926.
4. Kivisild., H.R. Hanging ice dams. In Proceedings of the 8th Congress International Association for Hydraulic Research, Montreal, QC, Canada, 24–29 August 1959; Volume 2.
5. Beltaos, S.; Dean, A.M. Field investigations of a hanging dam. In Proceedings of the IAHR Symposium on Ice, Quebec, QC, Canada, 27–31 July 1981.
6. Beltaos, S. Ice Cover Formation. In *River Ice Formation*; Beltaos, S., Ed.; Committee on River Ice Processes and the Environment, Canadian Geophysical Union, Hydrology Section: Edmonton, AB, Canada, 2013; pp. 181–251.
7. Sui, J.; Hicks, F.M.; Menounos, B. Observations of river bed scour under a developing hanging dam. *Can. J. Civ. Eng.* **2006**, *33*, 214–218. [CrossRef]
8. Shen, H.T.; Wang, D.S. Under cover transportation and accumulation of frazil granules. *ASCE J. Hydraul. Eng.* **1995**, *121*, 184–195. [CrossRef]
9. Gold, L.W.; Williams, G.P. An unusual ice formation on the Ottawa River. *J. Glaciol.* **1961**, *4*, 569–573. [CrossRef]
10. Gebre, S.; Alfredsen, K.; Lia, L.; Stickler, M.; Tesaker, E. Review of Ice Effects on Hydropower Systems. *J. Cold Reg. Eng.* **2013**, *27*, 196–222. [CrossRef]
11. Vergeynst, J.; Morse, B.; Turcotte, B. Quantifying frazil production, transport and deposition in a gravel-bed river: Case study of the St. Raymond hanging dam. *Cold Reg. Sci. Technol.* **2017**, *141*, 109–121. [CrossRef]
12. Hopper, H.R.; Raban, R.R. Hanging dams in the Manitoba Hydro system. In Proceedings of the Workshop on River Ice, Burlington, ON, Canada, 23–24 September 1980; pp. 195–208.
13. Zbigniewicz, H.S. Lake Winnipeg Regulation Ice Stabilization Program. In Proceedings of the Workshop on River Ice, Fredricton, NB, Canada, 24–26 September 1997; pp. 43–53.
14. Lees, K.; Clark, S.P.; Malenchak, J.; Chanel, P. Characterizing ice cover formation during freeze-up on the regulated Upper Nelson River, Manitoba. *J. Cold Reg. Eng.* **2021**, *35*, 04021009. [CrossRef]
15. Bourgault, D.; Richards, C.; Pawlowicz, R. A Matlab Package for Georectifying Oblique Digital Images (g rect). Retrieved from GitLab. Available online: http://demeter.uqar.ca/g_rect/index.php/A_Matlab_package_for_georectifying_oblique_digital_images_(g_rect) (accessed on 10 May 2023).
16. *ImageJ (Version 1.51) [Computer Software]*; National Institutes of Health and Laboratory for Optical and Computational Instrumentation (LOCI), University of Wisconsin: Madison, WI, USA, 2018.
17. *Agisoft Metashape Professional Edition (Version 1. 5) [Computer Software]*; Agisoft LLC.: St. Petersburg, Russia, 2019.
18. Senarathbandara, R.; Clark, S.P.; Dow, K. Investigating the effect of incoming ice supply rate on hanging dam formation. In Proceedings of the 22nd Workshop on the Hydraulics of Ice Covered Rivers, Canmore, AB, Canada, 9–13 July 2023.
19. Launder, B.E.; Rodi, W. The turbulent wall jet. *Prog. Aerosp. Sci.* **1981**, *19*, 81–128. [CrossRef]
20. Clark, S.P.; Wall, A. Freeze-up monitoring on the Dauphin River, Manitoba, Canada. In Proceedings of the 23rd International Symposium on Ice, Ann Arbor, MI, USA, 31 May–3 June 2016.
21. KGS Group; North/South Consultants. *Emergency Reduction of Lake Manitoba and Lake St. Martin Water Levels*; Manitoba Infrastructure and Transportation: Winnipeg, MB, Canada, 2014.
22. Wazney, L.E. Investigation of River Ice Cover Formation Processes at Freeze-Up. Ph.D. Thesis, University of Manitoba, Winnipeg, MB, Canada, 2019.
23. USGS Sentinel-2 EarthExplorer. Available online: https://apps.sentinel-hub.com/sentinel-playground (accessed on 7 June 2023).
24. USGS Landsat EarthExplorer. Available online: https://earthexplorer.usgs.gov (accessed on 8 June 2023).
25. Groeneveld, J.; Malenchak, J.; Morris, M. Numerical Model Studies of Ice Conditions during the Design and Construction of the Keeyask Generating Station. In Proceedings of the 19th Workshop on the Hydraulics of Ice Covered Rivers, Whitehorse, YT, Canda, 9–12 July 2017.